Simulation-Based Assessment of Rear Effect to Ballistic Helmet Impact

Jingzhou (James) Yang and Jichang Dai

Texas Tech University, james.yang@ttu.edu, jichang.dai@ttu.edu

ABSTRACT

Ballistic impact is one of the major causes for traumatic brain injury (TBI) and ballistic helmets are designed to provide protection from TBI. In real life, it is impossible to use real human subjects for experiments. Therefore, simulation based-methods are convenient to assess the rear effect to ballistic helmet impact and can provide crucial insights to injury. Rear effect happens when the interior of helmet is deformed and contacts with the human head. This paper proposes a simulation-based method to study the rear effect by using Head Injury Criterion (HIC) when the ballistic helmeted headform is impacted by a bullet with different impact angles and at various impact positions. Commercial software package LS-DYNA is employed to simulate the impact. A high fidelity headform model including detailed skull and brain has been used for the simulation purpose. Helmet and bullet are modeled according to the real shapes. The results show that, with a larger impact angle, the HIC score is smaller and therefore there is less damage to the brain. Based on the HIC scores obtained from the impact simulations at various impact positions, the bullet from back is the most dangerous position to the wearer.

Keywords: traumatic brain injury, ballistic helmet, high fidelity headform model.
DOI: 10.3722/cadaps.2010.59-73

1 INTRODUCTION

Helmets, which include military helmets, motorcycle helmets, sport helmets, emergency service helmets and more, can protect the wearers from head injuries. Significant research work has been done on numerical simulations of mainly motorcycle helmets [25], [14], [22], [18. There is an important difference between the impacts to motorcycle helmets and ballistic helmets: the former one is usually relative low velocity and high masses while the later is high velocity and low masses. A ballistic helmet is able to stop handgun bullets and rifle bullets in some cases. However, the shell of the helmet is still deformed and this deformation can cause a contact between the inside of the helmet and the head. This contact may cause head tissue injury and is known as “Rear Effect” [7], [16. Fig. 1 shows the deformations on the exterior and interior surface of a steel helmet.

Van Hoof et al. [28] analyzed the response of woven composite helmet material both experimentally and numerically. They performed the ballistic impact tests on flat panels consisting of the same material as ballistic helmets. LS-DYNA was used to predict the penetration and backplane response. The Van Hoof group continued their work to evaluate the ballistic impact response of composite helmet numerically in 2001 by using the previously presented model. It was found that the

helmet interior exhibited higher deformation than the flat panels and the global motion of the helmet was negligible. Ballistic impact on the helmeted head was analyzed. The simulation results showed that the helmet deformation can exceed the stand-off, resulting in an impact of the helmet interior with the skull.

Fig. 1: Deformations on the exterior and interior surface of a steel helmet.

Baumgartner and Willinger [3] studied the rear effect caused by a steel bullet launched at high velocity towards the helmet of military personnel. Their FE model included the human's head principal anatomical components and a helmet model made from an aluminum plate subjected to impact by a steel bullet. Pressure, Von-Mises stress, global strain energy, and force were calculated.

Aare and Kleiven [1] studied how different helmet shell stiffness affects the load levels in the human head during impacts, and how different impact angles affect the load levels in the human head. The studied data from the FE simulations were stress in the cranial bone, strain in the brain tissue, pressure in the brain, change in rotational velocity, and translational and rotational acceleration. They concluded that dynamic helmet shell deflections larger than the initial distance between the shell and the skull should be avoided to prevent the rear effect.

Tham et al. [26] carried out experiments and AUTODYN-3D simulations on the ballistic impact of a KEVLAR helmet. Also two ballistics test standards for KEVLAR helmet are simulated. Results from the simulations show that KEVLAR helmet is able to defeat a 9mm full-jacketed bullet traveling at 358 m/s.

Qiu [24] studied the rear effect by studying the human head response to the deformation caused by the ballistic impact to the frontal and side of the KEVLAR helmet. The studied data from the finite element simulations were stress in the cortical bone, pressure in the brain, and translational acceleration of the head.

Othman [21] determined the effect of the modulus of elasticity and the shear modulus of composite materials on ballistic resistance. Apart from that, the deformation and energy distribution of the helmet when struck by a bullet at velocity of 360m/s is also analyzed. In addition, the ballistic limit of the helmet made of four different types of composites namely Carbon fiber-reinforced Polyester, Glass fiber-reinforced Polyester, Kevlar fiber-reinforced Polyester, and Kevlar 29 fiber-reinforced Phenol are determined as well as the failure mechanism that occurred on the ballistic helmet.

In this work, a comprehensive simulation on the "Rear Affect" was carried out. A high fidelity headform model including scalp, skull, and brain was implemented in this simulation. The simulation considers different impact angles and the different positions of helmet, which are the front, side, top, and back part of the helmet. In addition, HIC with different bullet impact angles and at various impact positions is used to assess the "Rear Effect".

The paper is organized as follows. In Section 2, the Head Injury Criterion is introduced. Then the finite element analysis procedure is stated in Section 3, which includes the modeling and material properties of the three different Finite Element Models: headform, bullet, and helmet. The results are given in Section 4 and conclusion and discussion is in Section 5.

2 THE HEAD INJURY CRITERION

The Head Injury Criterion is a wildly accepted measure of the likelihood of the head injury arising from an impact released by National Highway Traffic Safety Administration (NHTSA) in 1972. It is based on the resultant translational acceleration. The formula is:

$$HIC = \left[\frac{1}{t_2 - t_1} \int_{t_1}^{t_2} a(t)\, dt \right]^{2.5} \left(t_2 - t_1 \right) \tag{1}$$

Where: a is the resultant translational acceleration at the centre of gravity. Unit: g

t1 and t2 =two points in time between which the acceleration acts. Unit: s

According to the time between t1and t2 (15 or 36 ms), HIC can be categorized to HIC15 and HIC36. HIC15 will be employed in this paper. At a HIC of 1000, one in six people will suffer a life-threatening injury to their brain, or more accurately, an 18% probability of a severe head injury, a 55% probability of a serious injury and a 90% probability of a moderate head injury to the average adult [17]. Fig. 2 shows the probability of specific head injury level for a given HIC score. It is based on the data from NHTSA [20]'s report and Prasad and Mertz [23]'s work. HIC(d) is used to correct the difference between the HIC for a full 50th percentile anthropometric test device and the free motion headform HIC [10]. The Formula is: HIC(d) =0.75446(HIC) +166.4.

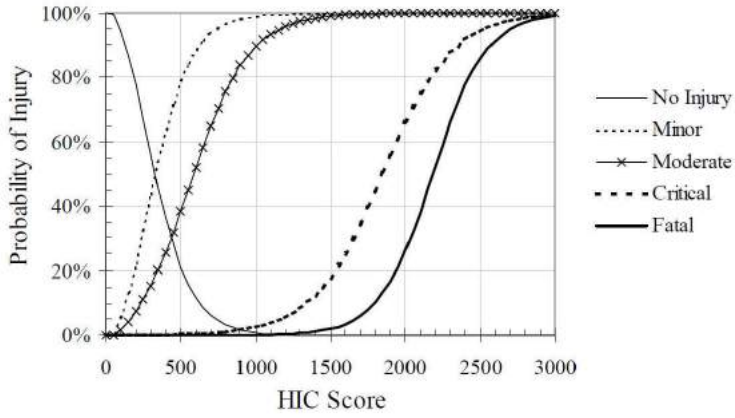

Fig. 2: Probability of specific head injury level for a given HIC score.

Critical, moderate, and minor head injuries are defined as the following (Canadian Playground Advisory):

Critical head injury – loss of consciousness for more than 12 hours with intracranial hemorrhaging; recovery uncertain; cerebral contusion; other neurological signs.

Moderate head injury – skull trauma with or without dislocated skull fracture and brief loss of consciousness; Fracture of facial bones without dislocation; deep wound(s).

Minor head injury – a skull trauma without loss of consciousness; superficial face injuries; fracture of nose or teeth.

3 FINITE ELEMENT ANALYSIS

This section will introduce the modeling processes and the material properties of the FE models which include headform, bullet, and helmet. The complete FE model is showed in Fig. 3. Note that skin is a really thin layer and relatively to the impact, the skin can be removed in the model and only the skeletal is considered.

Fig. 3: The complete FE model includes headform, helmet, and bullet.

3.1 Headform

The 3D shapes of the skull and brain are reconstructed from cross section images of the Visible Human Dataset (NIH). And the reconstructed 3D triangular surfaces are then remeshed to obtain boundary meshes with good quality for the consequent volumetric meshing as shown in Figure 4. The volumetric meshing is performed in the newest version of CFD-GEOM software from CFDRC (Version 2009, with the new capability of generating unstructured mesh for domain enclosed by discrete triangular surfaces) in Fig. 5. The total element number of skull is 179,752 and 135,144 for brain. The material properties are showed in Table 1 [12].

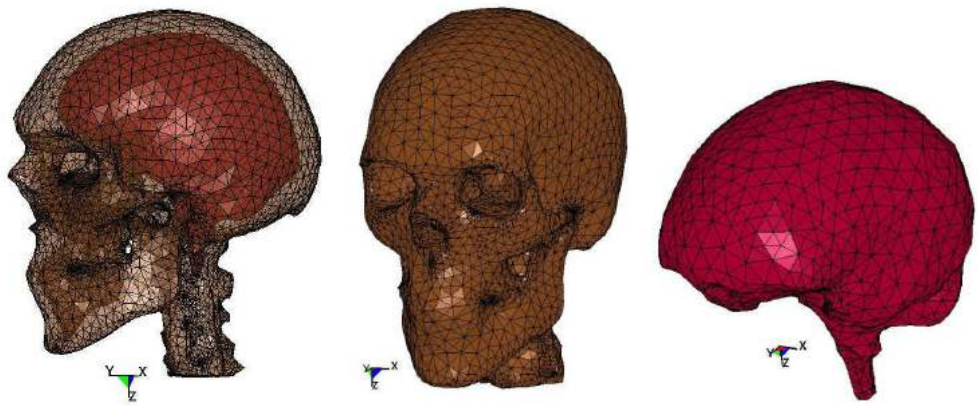

(a) (b) (c)

Fig. 4: The meshed models: (a) the skull and brain; (b) the skull; (c) the brain.

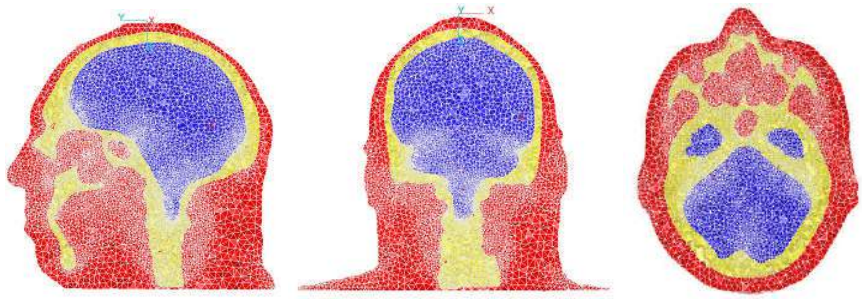

(a) (b) (c)

Fig. 5: The cross section view of generated unstructured volumetric meshes for scalp, skull, and brain. (a) The side view; (b) the front view; and (c) the top view.

Part	Material Model	Density (Kg/m^3)	Young's Modulus (N/m^2)	Poisson's ratio
Skull	Elastic	1800	8.75e9	0.26
Brain	Elastic	2000	6.7e6	0.49

Tab. 1: The material properties of skull and brain.

3.2 Bullet

The bullet is modeled as the 9x19 mm parabellum in Fig. 6, which is the world's most popular and widely used military handgun cartridge [2]. It has a mass of 8 gram and is assumed to have a velocity 360 m/s when it hits the helmet surface. The total element number is 5,504.

Fig. 6: The FE model of bullet.

The structure of bullet is assumed solid 4340 steel rather than a copper shell and lead core. A plastic kinematic hardening material model is used to represent the bullet with the material properties in Table 2 [15].

Strain rate in the plastic kinematic hardening model is accounted for using the Cowper-Symonds model to scale the yield stress as shown below [11]:

$$\sigma_Y = \left[1 + \left(\frac{\dot{\varepsilon}}{C}\right)^{\left(\frac{1}{P}\right)}\right]\sigma_0 \qquad (2)$$

where σ_0 is the initial yield stress, $\dot{\varepsilon}$ is the strain rate. When equivalent plastic strain of the element reaches the failure strain ε_f, part of the bullet in the bullet model in LS-DYNA disappears.

Modulus of elasticity, E (MPa)	Density, ρ (Kg/m3)	Poisson's ration, ν	Yield stress, σ_Y (MPa)	Tangent modulus, ET (MPa)
210 000	7850	0.3	792	21 000
Strain rate parameter, C		Strain rate parameter, P		Failure strain, ε_f
40		5		0.15

Tab. 2: The plastic kinematic hardening material properties of 4340 steel for bullet.

3.3 Helmet

The helmet is modeled as the geometry similar to the US Personal Armor System Ground Troops' (PASGT), North Atlantic Treaty Organization (NATO) standard in Fig. 7. The total element number is 11,175. The thickness of shell is 8mm. The total mass of helmet is 1.15Kg similar to most of the helmets in the market. The interior equipment is not modeled since they have a small influence on the interaction between the shell and skull [1] and the Swedish National Police Board performs many of their helmet tests without the interior gears. In these tests performed in Beschussamt Mellrichstadt, the helmet shell was cleared from all interior equipments and the shell itself was put on a fixture without constrains. [4].

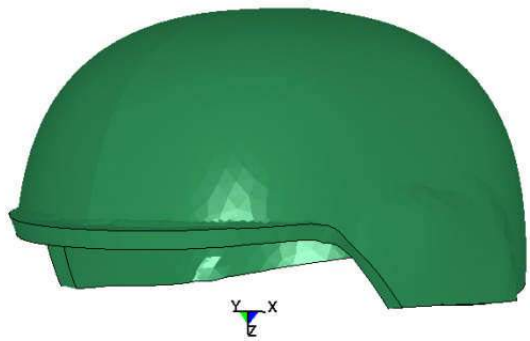

Fig. 7: The FE model of helmet.

The Chang-Chang composite failure material model [8], [9] is used to represent the Kevlar helmet with the material properties in Table 3[9].

4 SIMULATION RESULTS

Different impact angles and impact positions were simulated and the results show that higher impact angles generated lower injury and the back impact from the helmet is the most dangerous position.

4.1 Impact Angles

In the battlefield, most of the bullets will not actually hit the surface of helmet perpendicularly. They more likely impact the helmet with an angle. Therefore, four different impact angles α are simulated

($\alpha_1 = 0^0$, $\alpha_2 = 22.5^0$, $\alpha_3 = 45^0$, $\alpha_4 = 67.5^0$) shown in Fig. 8. Because on the different parts of the helmet has the similar pattern in the results, we only show the results for the front part of helmet.

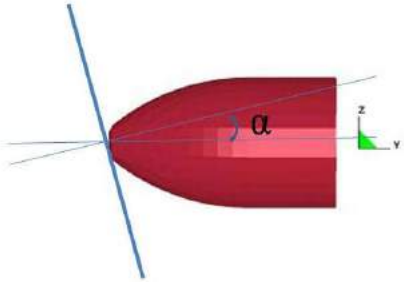

Fig. 8: The impact angle α when the bullet hit the helmet.

Fig. 9 shows the impact processes when the bullet strikes the helmet with different angles. When the bullet hits the helmet with a larger angle, the bullet has smaller deformation and less kinetic energy is transferred to the head. The results shown in Table 4 illustrate that impact angles have a great effect on the head response and deflection of the helmet. A larger angle significantly reduces the maximum v-m stress on skull bone, which is shown in Fig. 10, as well as the absolute values of the maximum/minimum pressure and maximum principal strain in the brain tissue. HIC scores given in Fig. 11 are not high enough to cause a head injury according to Fig. 2 and decrease with the increasing of the impact angle.

Density, ρ (GPa)	1440	Longitudinal tensile strength along a-axis (GPa)	2.886
Young's modulus in a-direction, Ea (GPa)	164	Transverse tensile strength along b-axis (GPa)	1.486
Young's modulus in b&c-direction, Ea=Ec (GPa)	3.28	Transverse compressive strength along b-axis (GPa)	1.7
Poisson ration, υ ba= υ ca= υ cb (GPa)	0	Normal tensile strength along c-axis (GPa)	1.486
Shear modulus, G_{ab} =G_{bc} = G_{ca} (GPa)	3.28	Transverse shear strength in ca-plane (GPa)	1.586
Shear strength in the ab plane (GPa)	1.88	Transverse shear strength in cb-plane (GPa)	1.886

Tab. 3: The Chang-Chang composite failure material model properties for Kevlar helmet.

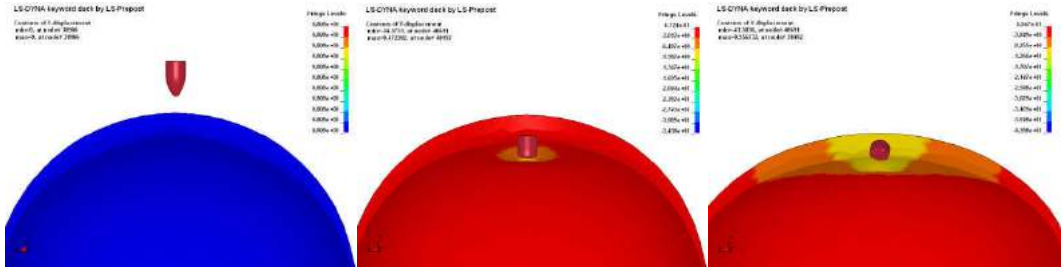

(a)

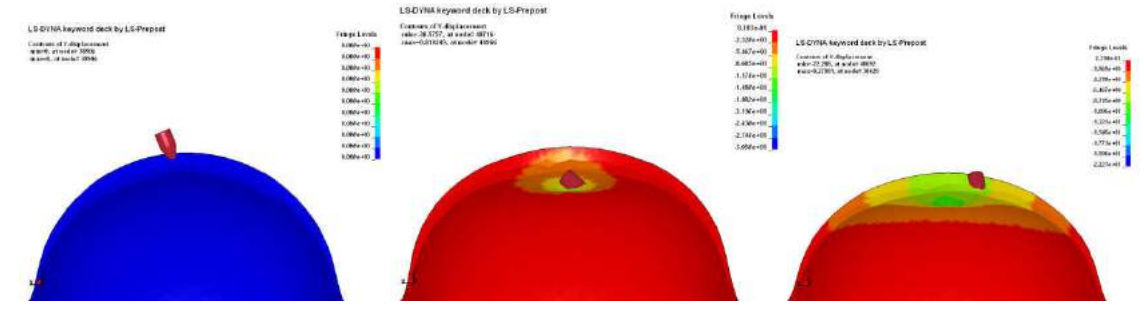

(b)

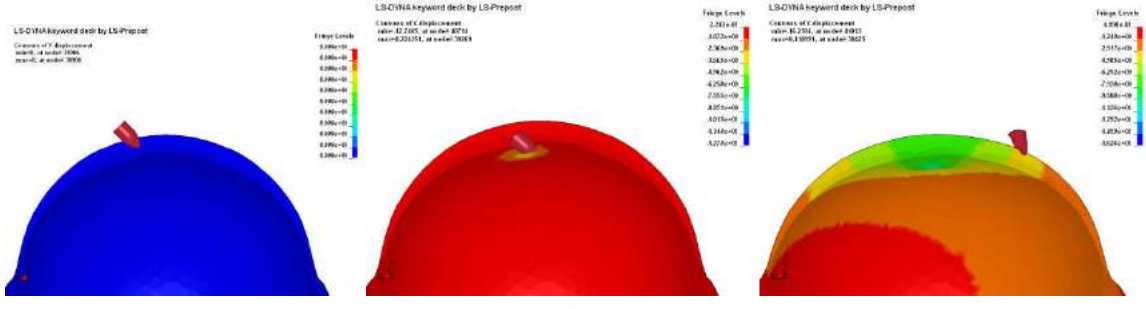

(c)

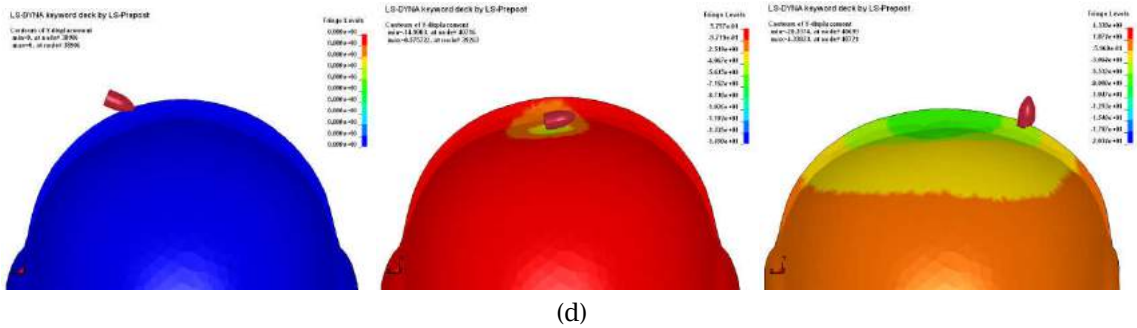

(d)

Fig. 9: The shell deflection with different impact angles: (a) Front 0º; (b) front 22.5º; (c) front 45º; (d) front 67.5º.

	Front 0º	Front 22.5º	Front 45º	Front 67.5º
Maximum von Mises stress in the skul bone (Mpa)	208	135	90	26
Maximum pressure in the brain (Mpa)	2.1	1.2	0.9	0.2
Minimum pressure in the brain (Mpa)	-1.8	-1.0	-0.7	-0.1
Maximum principal strain in the brain	2.1	1.8	1.6	0.2
Helmet shell deflection (mm)	13	12	11	8

Tab. 4: The results from different impact angle at front part of helmet.

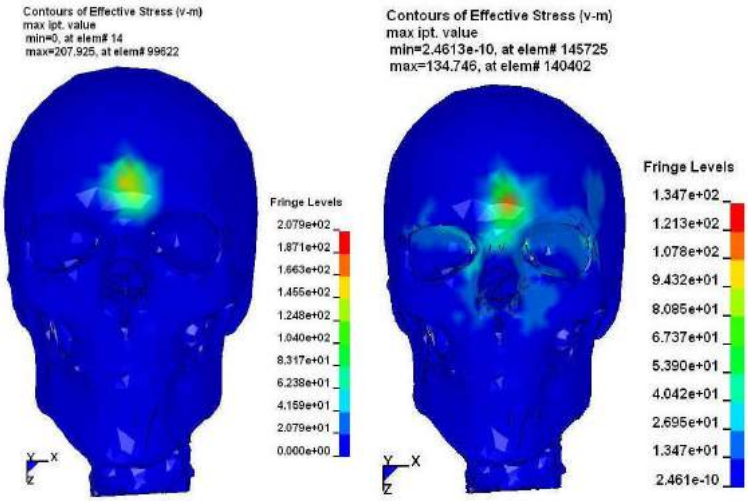

(a) 0º (b) 22.5º

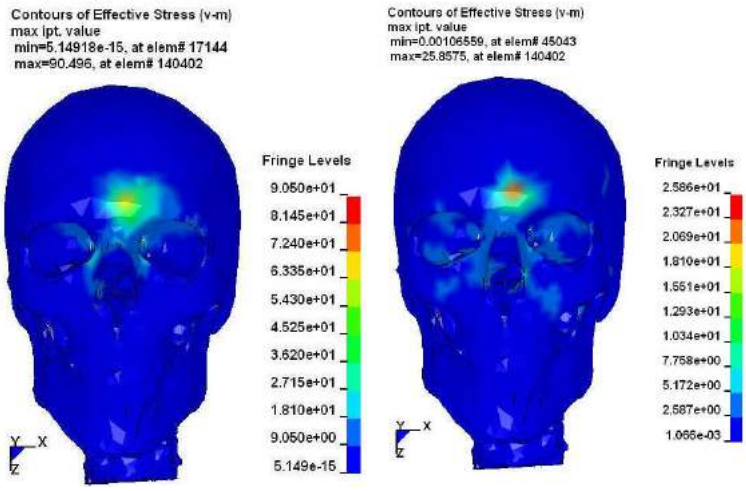

(c) 45º (d) 67.5º

Fig. 10: The Von Mises stress distributions on skull when is the bullet hits the helmet with different impact angles.

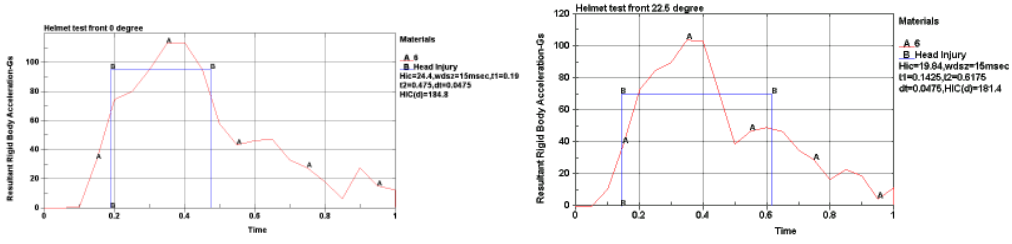

(a) 0º (b) 22.5º

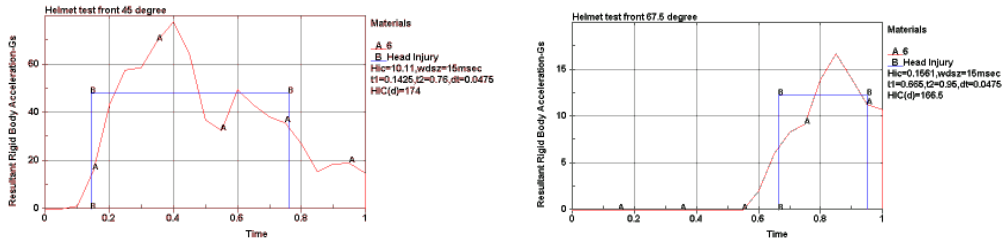

(c) 45º (d) 67.5º

Fig. 11: The HIC scores from different impact angles.

4.2 Impact Positions

Four impact positions of the helmet with the 0 degree impact angle shown in Fig. 12 (front, side, top and back) are simulated.

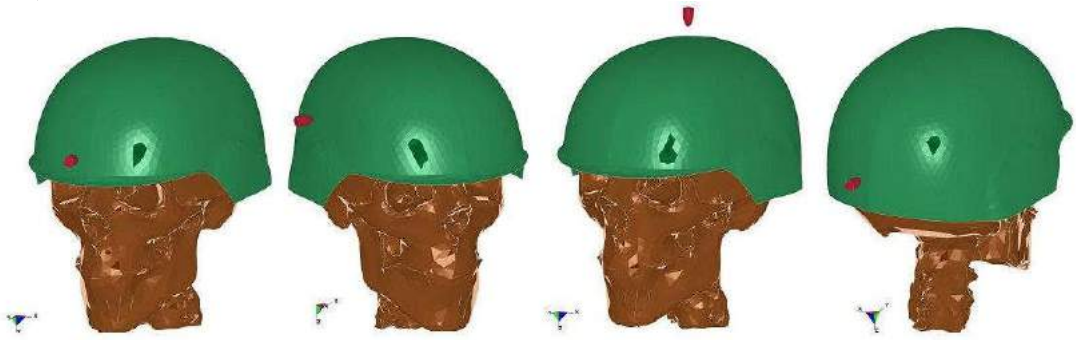

(a) (b) (c) (d)

Fig. 12: Impact positions: (a) Front; (b) side, (c) top; and (d) back.

Fig. 13 shows the simulation results (the maximum v-m stress on the skull bone) of different impact positions. The maximum/minimum pressure and the maximum principal strain in the brain tissue are shown in Table 5. Fig. 14 shows that the impact from the back part of the helmet generated the highest HIC score 54.52, though it is not high enough to cause a head injury. Fig. 15 shows the Von Mises stress on the skull at different time steps when the helmet is impacted at the back part by a bullet. The bullet that comes from the top has a HIC score of 38.24, which is more dangerous than that from the front which has a HIC score of 24.4. When the helmeted head is hit by a bullet from the side part, the HIC is the lowest 10.16. The HIC scores only depend on the resultant translational acceleration. However, it is not necessary that the HIC scores have the same trend as the values of Von Mises stress, maximum/ minimum brain pressure or maximum principal strain in the brain.

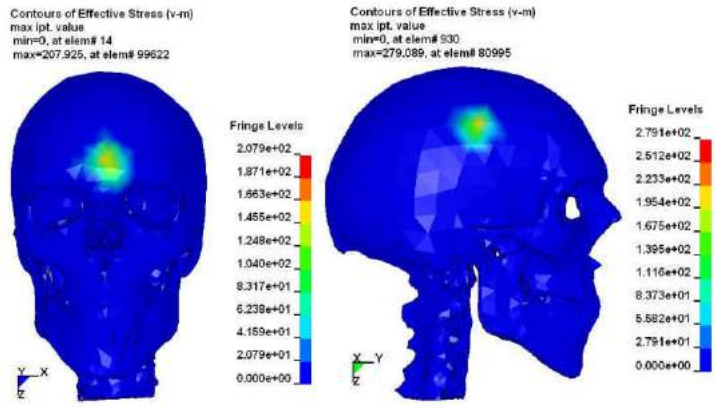

(a) Front (b) Side

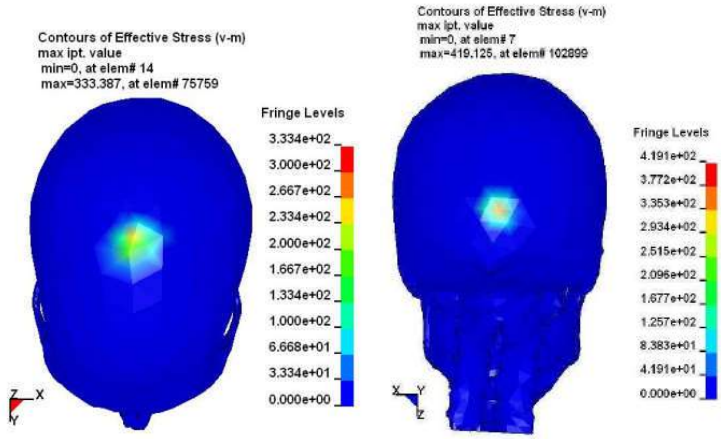

(b) Top (d) Back

Fig. 13: The Von Mises stress distributions on skull when it is hit at different positions.

	Front 0º	Side 0º	Top 0º	Back 0º
Maximum Von Mises stress in the skul bone (Mpa)	208	279	333	419
Maximum pressure in the brain (Mpa)	2.1	5.8	7.8	6.5
Minimum pressure in the brain (Mpa)	-1.8	-4.3	-6.5	-4.9
Maximum principal strain in the brain	2.1	4.3	7.3	5.8
Helmet shell deflection (mm)	13	12	11	14

Tab. 5: The results from different impact angle at front part of helmet.

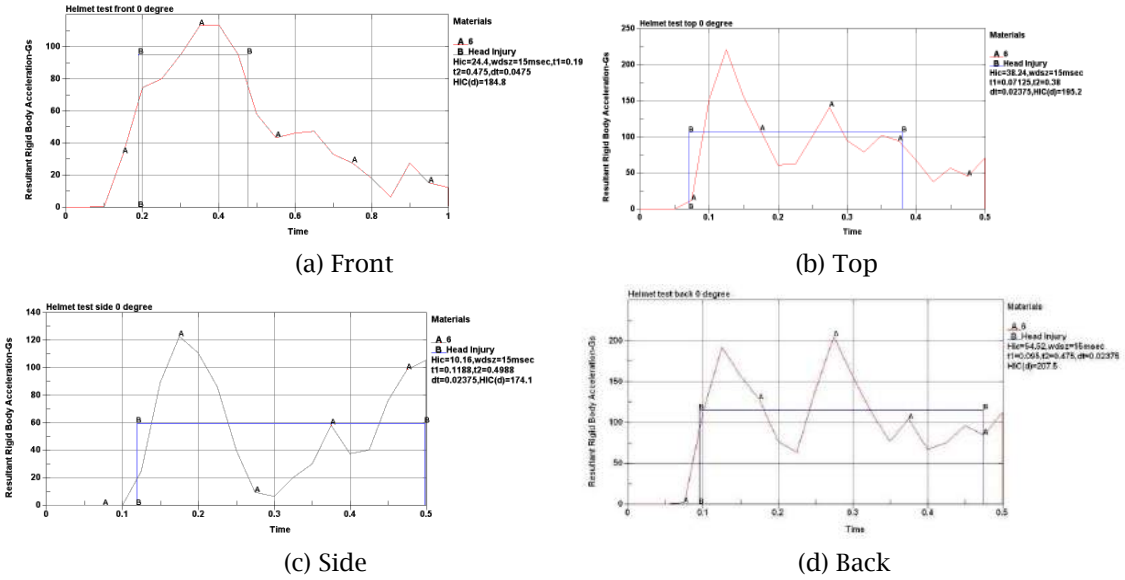

(a) Front (b) Top

(c) Side (d) Back

Fig. 14: The HIC scores from different impact positions.

4.3 Validation

Although the real shooting test is not available for this research, the literatures reveal some similar conclusions. In Aare and Kleiven's work, their human head FE model was validated against impact tests on cadavers and helmet models were validated by shooting tests. They also conducted a study on different bullet impact angles. The result shows different maximum Von Mises stress values from our work since the different helmet model, but the same trend: the larger impact angle, the less damage to the head.

5 CONCLUSION AND DISCUSSION

A high fidelity headform model has been implemented in the ballistic impact simulation to a helmet in LS-DYNA environment. Various parameters have been investigated to better understand the ballistic helmet impact. HIC criterion has been used to assess the head injury. Simulation studies have shown that the both the impact angle and impact position have great effect on the HIC score. With a larger impact angle, the bullet will more likely skid over the surface of helmet and have less kinetic energy transferred to the helmet. When the bullet hits the back part of helmet, the largest HIC score, 54.52, has been observed compared to the situations when the bullet hits the other parts which are: 38.24 for the top; 24.40 for the front; 10.16 for the side. However, the HIC scores are not necessary to have the same trend as the values of Von Mises stress, maximum/minimum brain pressure or maximum principal strain in the brain because the HIC only depends on the resultant translational acceleration. As in Fig. 16, different positions of human head have non-uniform thickness distribution and the thickest part is the forehead. Therefore, Von Mises stress, maximum/minimum brain pressure, and maximum principal strain in the brain are all the smallest when the helmet is impacted at the front part compared with the other three situations.

This work has several assumptions and limitations. For the head model, soft tissues over the skull, like the muscle and skin, were not considered. The skull and brain were modeled as linear elastic isotropic material to simplify the problem. In the future work, the skull will be modeled as laminated material, and the brain should be viscoelastic material. For the bullet model, it was modeled as a whole solid material instead of the real structure including a copper jacket and a lead core. The plastic kinematic hardening material model instead of the Johnson-Cook material model [13] that can better describe the large and rapid deformation was used for the bullet. Therefore, the deformation of bullet

is not the same as the observation from actual shooting test. For the helmet model, more accurate material properties are needed and helmet accessories like the chin strap will be added in the future model.

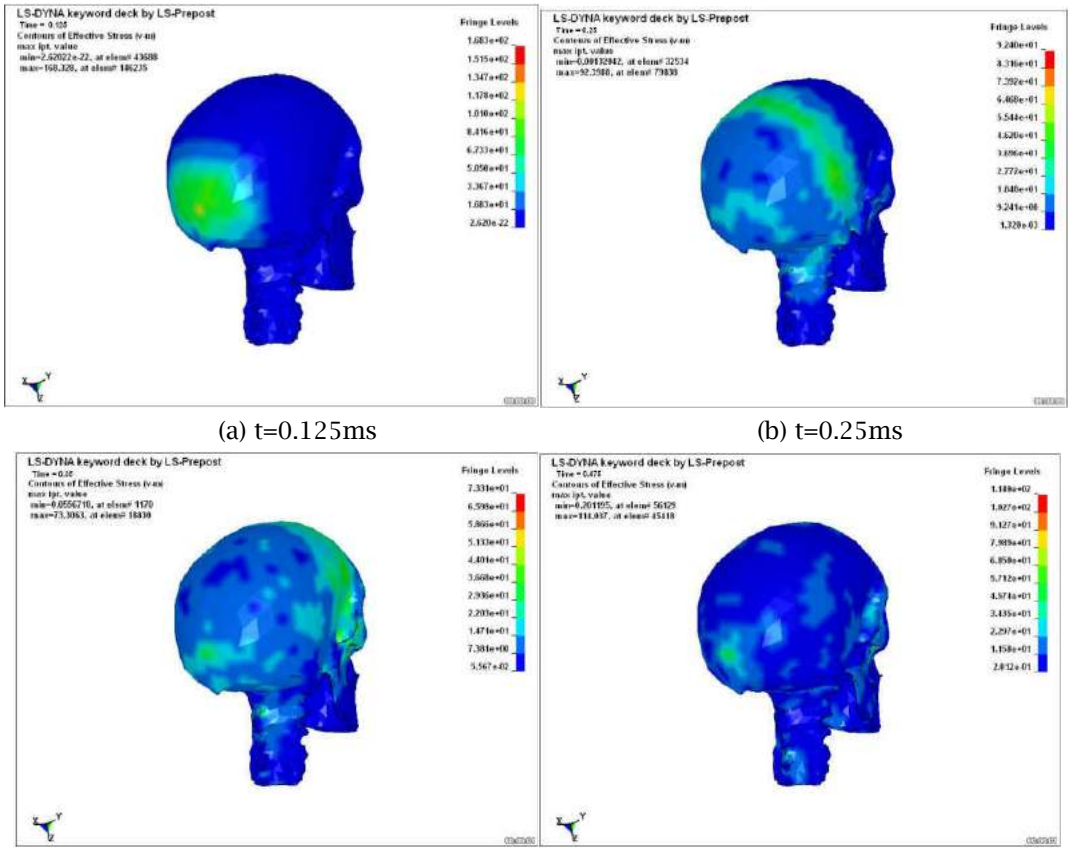

(a) t=0.125ms (b) t=0.25ms

(c) t=0.35ms (d) t=0.475ms

Fig. 15: The Von Mises stress distributions at different time steps on skull hit from the back.

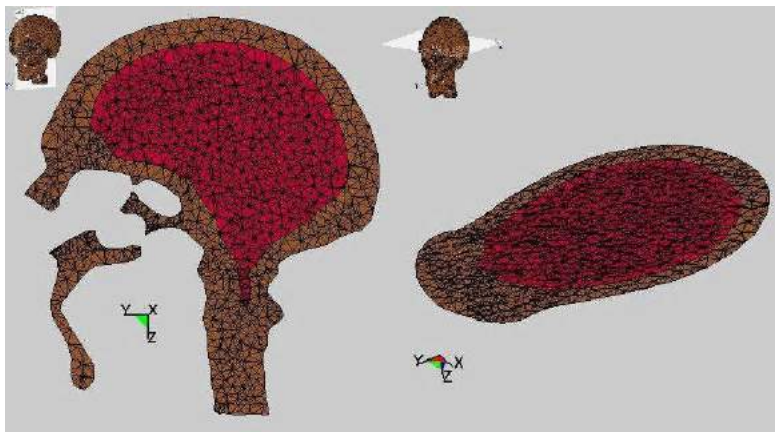

Fig. 16: The distribution of skull thickness of the human head.

ACKNOWLEDGEMENTS

This research was partly supported by the startup fund of Texas Tech University.

REFERENCES

[1] Aare, M.; Kleiven, S.: Evaluation of head response to ballistic helmet impacts, using FEM, International Journal of Impact Engineering, 34, 2007, 596–608.
[2] Barnes, F.: Skinner, Stan. ed. Cartridges of the World. 11th Edition. Cartridges of the World. Gun Digest Books, 2006, p. 295, ISBN 978-0-89689-297-2.
[3] Baumgartner, D.; Willinger, R.: Finite element modeling of human head injuries caused by ballistic projectiles, Proc. RTO Specialist Meeting, the NATO, Koblenz, Germany, 2003.
[4] Beschussamt Mellrichstadt.: March 2001. Test Protokoll-Nr: 01M072-01, Date: 21.03.2001; 01M073A01, 21.03.2001; 01M079-01, 29.03.2001;01M085A01, 30.03.2001; 01M085B01, 30.03.2001, Bericht-No: 140-143, Date: 19.03.2001; Beschussamt Mellrichstadt, Lohstrasse 5,97638 Mellrichstadt, Germany.
[5] Canadian Playground Advisory Inc. Risk of head injury and HIC scores. http://www.playgroundadvisory.com/.
[6] http://www.nlm.nih.gov/research/visible/visible_human.html.
[7] Carroll, A.; Soderstrom, C.: A new non-penetrating ballistic injury, Ann Surg., 188, 1978, 753–7.
[8] Chang, F. K.; Chang, K. Y.: Post-Failure Analysis of Bolted Composite Joints in Tension or Shear-Out Mode Failure, J of composite material, 21, 1987, 809-833.
[9] Chang, F. K.; Chang, K. Y.: A Progressive Damage Model for Laminated Composites Containing Stress Concentrations, Journal of Composite Materials, 21, 1987, 834-55.
[10] Fox, D. M.: Energy Absorber for Vehicle Occupant Safety and Survivability. USA TACOM 6501 E 11 Mile Road Warren, MI 48397-5000, 2006.
[11] Hallquist, J. O.: LS-DYNA Theoretical Manual, Livermore Software Technology Corporation, Livermore, CA, 1997.
[12] Horgan, T. J.: A Finite Element Model of the Human Head for Use in the Study of Pedestrian Accidents, In Department of Mechanical Engineering, University College Dublin, Doctor of Philosophy: 138-140. National University of Ireland, 2005.
[13] Johnson, G. R.; Cook, W. H.: A Constitutive Model and Data for Metals Subjected to Large Strains, High Strain Rates and High Temperatures. Presented at the Seventh International Symposium on Ballistics, The Hague, The Netherlands, 1983.
[14] Kostopoulos, V.; Markopoulos, Y. P.; Giannopoulos, G.; Vlachos, D. E.: Finite element analysis of impact damage response of composite motorcycle safety helmets, Composites: part B 33, 2002, 99-107.
[15] Kurtaran, H.; Buyuk, M.; Eskandarian, A.: Ballistic Impact Simulation of GT Model Vehicle Door Using Finite Element Method, Theoretical and Applied Fracture Mechanics, 40(2), 2003 113-121.
[16] Liden, E.; Berlin, R.; Janzon, B.; Schantz, B.; Seeman, T.: Some observations relating to behind-body armor blunt trauma effects caused by ballistic impact, J Trauma. 27(suppl 1), 1988, S145–8.
[17] Mackay, M.: The Increasing Importance of the Biomechanics of Impact Trauma, Sadhana. Vol. 32, Part 4, 2007, 397–408.
[18] Mills, N. J.; Gilchrist, A.: Finite-element analysis of bicycle helmet oblique impacts, International Journal of Impact Engineering 35, 2008, 1087–1101.
[19] National Highway Traffic Safety Administration (NHTSA), Department of Transportation (DOT), (1972). Occupant Crash Protection – Head Injury Criterion S6.2 of MVSS 571.208, Docket 69-7, Notice 17. NHTSA, Washington, DC.
[20] NHTSA, Final Economic Assessment, FMVSS No. 201, Upper Interior Head Protection, 1995.
[21] Othman, R. B.: Finite Element Analysis of Composite Ballistic Helmet Subjected To High Velocity Impact, Master's Thesis. Universiti Sains Malaysia, 2009.
[22] Pinnojil, P. K.; Mahajanl, P.: Finite element modeling of helmeted head impact under frontal loading, Sadhana Vol. 32, Part 4, 2007, 445–458.
[23] Prasad, P.; Mertz, H. J.: The Position of the United States Delegation to the ISO Working Group on the Use of HIC in the Automotive Environment. SAE # 851246, Society of Automotive Engineers, 1985.

[24] Qiu, Z. X.; AM17 Protective Functional Evaluation of Helmet against Ballistic Impact. Bachelor's Thesis, National University of Singapore, 2007/2008.
[25] Shuaib, F. M.; Hamouda, A. M. S.; Umar, R. S. R.; Hamdan, M. M.; Hashmi, M. S. J.: Motorcycle helmet Part I. Biomechanics and computational issues. Journal of materials Processing Technology, 123, 2002, 406-421.
[26] Tham, C. Y.; Tan, V. B. C.; Lee, H. P.: Ballistic impact of a KEVLARs helmet: Experiment and simulations, International Journal of Impact Engineering. 35, 2008, 304–318.
[27] Van Hoof, J.; Deutekom, M. J.; Worswick, M. J.; Bolduc, M.: Experimental and numerical analysis of the ballistic response of composite helmet materials, 18th International symposium on ballistics, San Antonio, TX, 1999.
[28] Van Hoof, J.; Cronin, D. S.; Worswick, M. J.; Williams, K. V.; Nandlall, D.: Numerical head and composite helmet models to predict blunt trauma, 19th International Symposium on ballistics, Interlaken, Switzerland, 2001.